Pictorial Essay | Neuroimaging and Head & Neck

https://doi.org/10.3348/kjr.2017.18.4.710
pISSN 1229-6929 · eISSN 2005-8330
Korean J Radiol 2017;18(4):710-721

Korean Journal of Radiology
KJR

Splenial Lesions of the Corpus Callosum: Disease Spectrum and MRI Findings

Sung Eun Park, MD[1], Dae Seob Choi, MD[1, 2], Hwa Seon Shin, MD[1], Hye Jin Baek, MD[1], Ho Cheol Choi, MD[1], Ji Eun Kim, MD[1], Hye Young Choi, MD[1], Mi Jung Park, MD[1]

[1]Department of Radiology, Gyeongsang National University School of Medicine, Jinju 52727, Korea; [2]Gyeongsang Institute of Health Science, Gyeongsang National University School of Medicine, Jinju 52727, Korea

The corpus callosum (CC) is the largest white matter structure in the brain, consisting of more than 200–250 million axons that provide a large connection mainly between homologous cerebral cortical areas in mirror image sites. The posterior end of the CC is the thickest part, which is called the splenium. Various diseases including congenital to acquired lesions including congenital anomalies, traumatic lesions, ischemic diseases, tumors, metabolic, toxic, degenerative, and demyelinating diseases, can involve the splenium of the CC and their clinical symptoms and signs are also variable. Therefore, knowledge of the disease entities and the imaging findings of lesions involving the splenium is valuable in clinical practice. MR imaging is useful for the detection and differential diagnosis of splenial lesions of the CC. In this study, we classify the disease entities and describe imaging findings of lesions involving the splenium of the CC based on our experiences and a review of the literature.

Keywords: *Brain; Corpus callosum; Magnetic resonance imaging*

INTRODUCTION

The splenium is the thickest and most posterior portion of the corpus callosum (CC). It consists of numerous axonal fibers that mainly connect both temporal, posterior parietal, and occipital cortices (1). However, until now, the exact function of the splenium of corpus callosum (SCC) is not well known. In addition, various congenital and acquired diseases can involve the SCC and their clinical signs and symptoms are also variable such as confusion, ataxia, dysarthria, and seizure (Table 1) (2-4). Therefore, the knowledge of the disease category and their imaging findings can be helpful for the accurate diagnosis of the SCC lesions.

Received October 15, 2016; accepted after revision December 18, 2016.

Corresponding author: Dae Seob Choi, MD, Department of Radiology, Gyeongsang National University Hospital, Gyeongsang National University School of Medicine, 79 Gangnam-ro, Jinju 52727, Korea.
• Tel: (8255) 750-8211 • Fax: (8255) 758-1568
• E-mail: choids@gnu.ac.kr

Normal Anatomy and Development

The CC is comprised of four parts: reflected anterior portion, the rostrum; the genu, anterior bulbar end; the splenium, posterior rounded end; and the body that lies between the genu and splenium. During the 8th and 20th weeks of gestation period, the CC is formed by development of the callosal precursors and the fibers from the cortices of both cerebral hemispheres. It develops anteriorly at the genu and proceeds posterior to the splenium except for the rostrum, which is the last area to show the crossed fibers (1, 5).

Korean Journal of Radiology
KJR

Table 1. Clinical Findings of Splenial Lesions of Corpus Callosum

Symptoms and Signs	%
Confusion	50–60
Ataxia	33–43
Dysarthria	13–43
Seizure	10–40
Headache	16–23
Hemiparesis	5–27
Increased muscle tone	7–16

Congenital Lesions

Agenesis: Complete vs. Partial

Agenesis is the most common congenital lesion of the CC. A wide range of developmental malformations can affect the CC, ranging in severity from total absence (complete agenesis) to lesser degrees of deficiency (partial agenesis) involving only the splenium. In the absence of the splenium, the occipital horns migrate superiorly

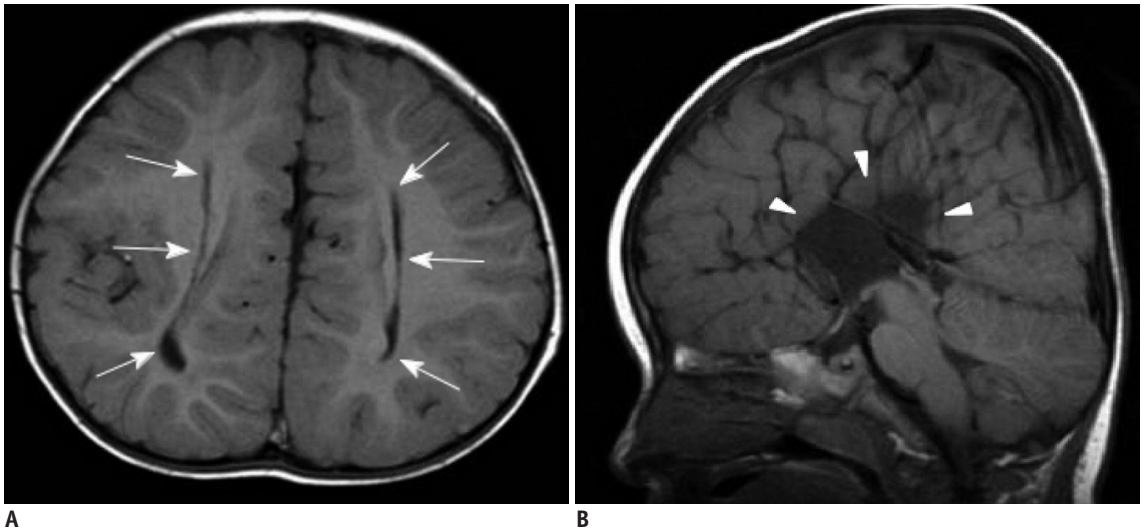

A B

Fig. 1. 1-year-old female patient with complete corpus callosal agenesis.
A. T1-weighted axial image shows parallel configuration of both lateral ventricles (arrows). **B.** T1-weighted sagittal image reveals complete agenesis of corpus callosum (arrowheads).

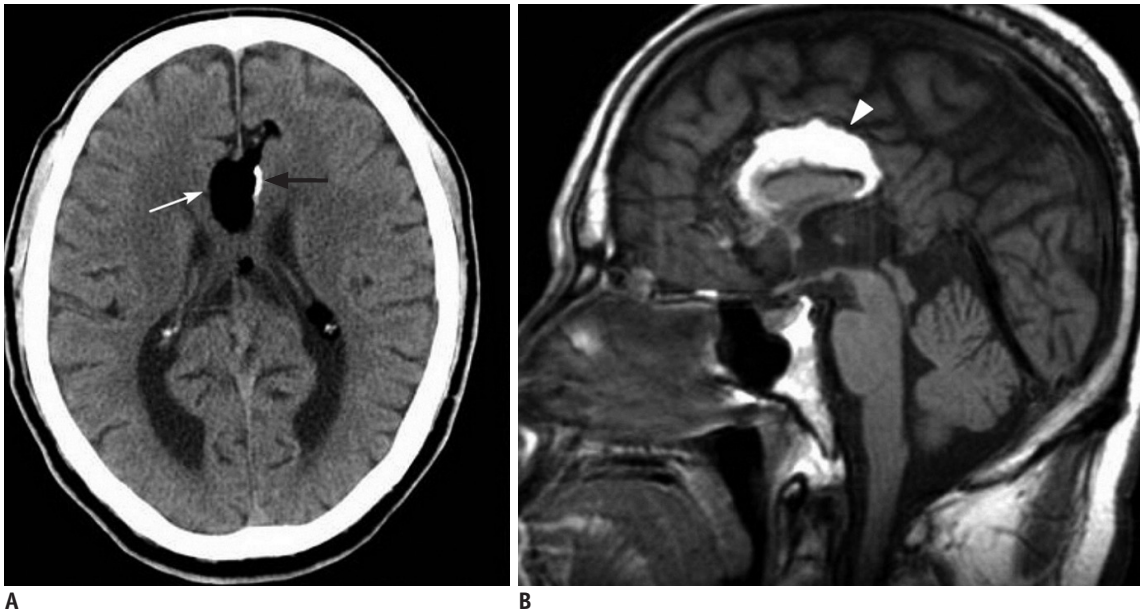

A B

Fig. 2. 70-year-old male patient with tubulonodular type pericallosal lipoma and partial corpus callosal agenesis.
A. Axial CT image shows tubulonodular type lipoma in frontal interhemispheric fissure (white arrow). There is linear calcification at left side of lesion (black arrow). **B.** Sagittal T1-weighted MR image reveals partial agenesis of corpus callosum and hyperintense pericallosal lipoma (arrowhead).

into the underdeveloped white matter (WM), resulting in the dilatation of the trigone and occipital and posterior temporal horns and its appearance is known as colpocephaly (Fig. 1) (5, 6).

Lipoma

Intracranial lipoma is a kind of congenital malformation, which arises from abnormal persistence or aberrant differentiation of the primitive meninx. Nearly 30–40% of intracranial lipomas occur in the pericallosal region. The morphology of pericallosal lipomas has been described by two types i.e., tubulonodular and curvilinear. Tubulonodular type lipomas are mostly located in the frontal lobe and commonly associated with agenesis of the CC (Fig. 2). On the contrary, curvilinear type lipomas are usually thin and rest around the SCC. Combined callosal malformations are

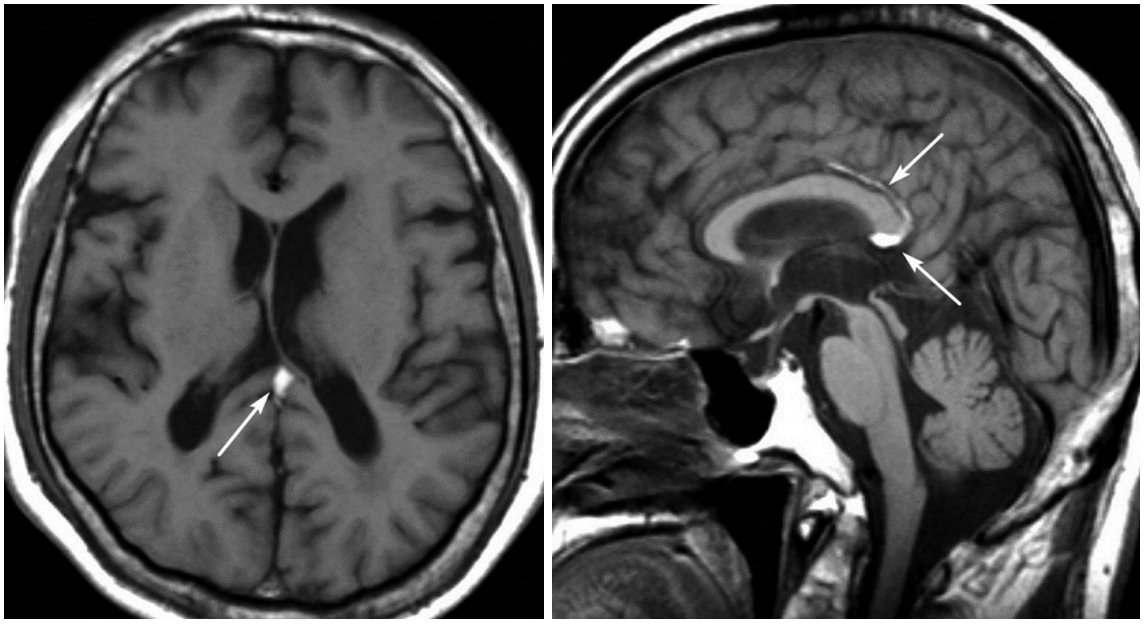

A B

Fig. 3. 64-year-old male patient with curvilinear type pericallosal lipoma and partial corpus callosal agenesis.
T1-weighted axial **(A)** and sagittal **(B)** images show hyperintense lipoma (arrows) superior and posterior to corpus callosum. Splenial portion is not fully developed.

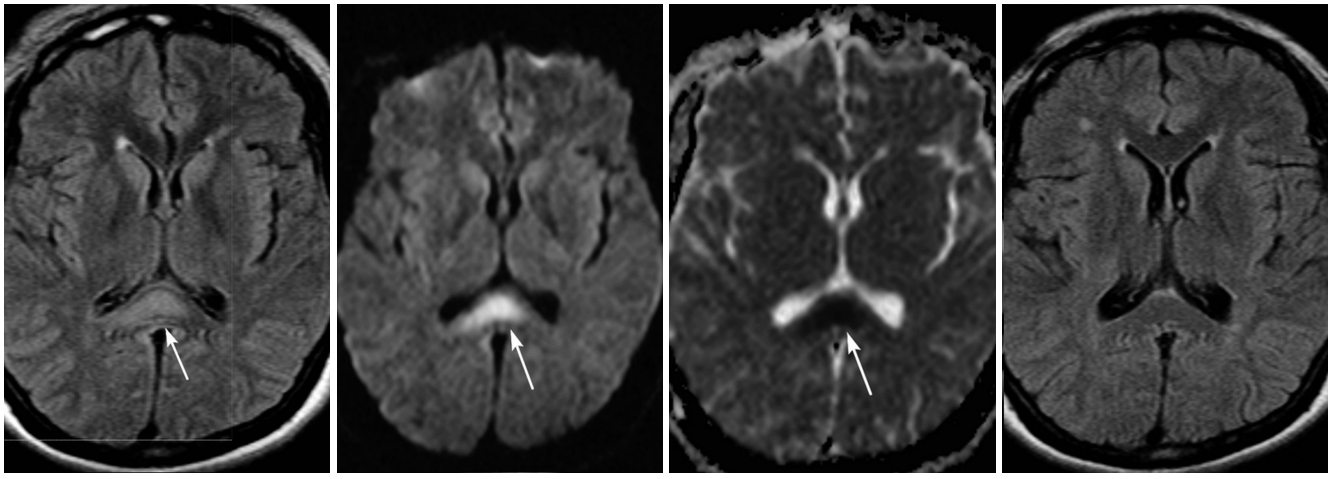

A B C D

Fig. 4. 29-year-old female patient with diffuse axonal injury lesion. Patient was involved in motor vehicle accident 9 days ago.
A, B. Axial FLAIR **(A)** and DWI **(B)** images show hyperintense lesion in splenial portion of corpus callosum (arrows). Lesion is more conspicuously demonstrated on DWI than on FLAIR image. **C.** ADC map image reveals restricted water diffusion of lesion (arrow). **D.** On follow-up FLAIR image obtained 17 months later, splenial lesion has disappeared. ADC = apparent diffusion coeffcient, DWI = diffusion-weighted image, FLAIR = fluid-attenuated inversion recovery

Korean Journal of Radiology
KJR

mild and uncommon (Fig. 3) (7, 8). Calcification is often accompanied with lipoma. It shows curvilinear, around the periphery of the lesion, or may be nodular within the center of the lesion (Fig. 2).

Lipomas are easily identifiable on MR imaging, with homogenous hyperintensities on T1-weighted images and loss of signal on fat-suppressed images.

Traumatic Lesions

Diffuse Axonal Injury

Diffuse axonal injury (DAI) is caused by traumatic shearing forces that occur when the head is rapidly accelerated, decelerated, or rotated. The major pathologic finding of DAI is the disruption of the axons. DAI most commonly affects the WM in areas including the brain stem and the CC. In addition, the cerebral corticomedullary junction, cerebral peduncles, basal ganglia, thalamus, and deep hemispheric nuclei are other main locations for DAI. The CC injuries are most common in the posterior body and splenium (9). DAI is the most common acquired lesion of the SCC. MR imaging is very useful for the detection of DAI lesions. Acute lesions show bright signal intensities on diffusion-weighted images (DWIs) with restricted water diffusion due to acute cell death (Fig. 4) (10). Chronic lesions are associated with hemosiderin and encephalomalacia. It is hypointense on T1 and hyperintense on T2-weighted image, surrounded by peripheral hypointense rim corresponding to the deposition of hemosiderin. DAI lesions are commonly associated with microhemorrhage that is most sensitively detected on gradient echo (GRE) T2* or susceptibility-weighted images as foci of dark signal intensity (5, 10-12).

Ischemic Lesions

Infarction

Because of the abundant blood supply from three main arterial systems and significant pericallosal anastomotic plexus between the main blood supplies, a focal infarction of the CC is rare. The splenium is the most common location of the CC infarction (13). On MR imaging, infarctions of the CC have the same features as infarctions elsewhere in the brain. In acute stage, they exhibit reduced diffusivity on DWI, followed by edema with high intensity on T2 and low intensity on T1-weighted imaging (Fig. 5). Area of gliosis and atrophy develop later (14, 15).

Hypoxic-Ischemic Encephalopathy

Hypoxic-ischemic encephalopathy frequently affects premature infants and is thought to represent watershed infarction in the setting of low flow or decreased oxygen states. Severe cases may involve the CC. MR is the most sensitive imaging technique for examining patients with suspected hypoxic-ischemic brain injury. Hypoxic-ischemic injury to the WM including the CC demonstrates T2 hyperintensity and T1 hypointensity due to ischemia-induced edema. In acute and early subacute stages, lesions demonstrate bright intensity on DWI with restricted water diffusion (Fig. 6). End-stage periventricular leukomalacia shows ventriculomegaly, loss of the periventricular WM with

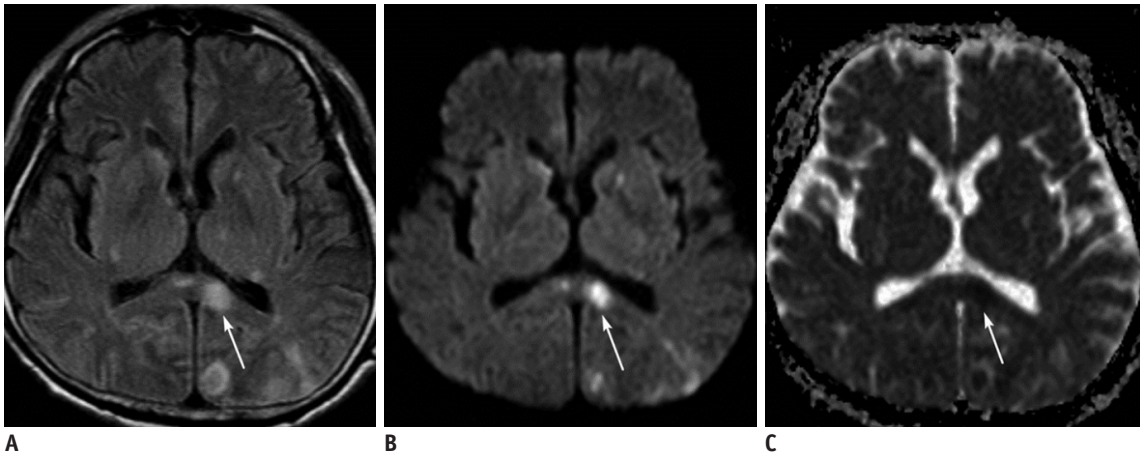

Fig. 5. 62-year-old male patient with acute splenial infarction.
A, B. Axial FLAIR image **(A)** and DWI **(B)** show multiple hyperintense lesions in bilateral basal ganglia, left thalamus, splenium of corpus callosum (arrows), and left occipital lobe. Splenial lesion (arrows) is more conspicuously demonstrated on DWI than on FLAIR image. **C.** ADC map image reveals restricted water diffusion of lesion (arrow). ADC = apparent diffusion coeffcient, DWI = diffusion-weighted image, FLAIR = fluid-attenuated inversion recovery

increased T2 signal and thinning of the CC (Fig. 6D) (15, 16).

Hypoglycemic Encephalopathy

Hypoglycemia is a medical emergency that involves an abnormal decrease in the serum glucose level. Overuse of insulin or oral hypoglycemic agents, or other medical conditions such as sepsis, renal or hepatic failure can cause hypoglycemia. Progression of hypoglycemia leads to symptoms of confusion and delirium. Critical symptoms as coma, irreversible brain damage or vegetative state can also occur in severe cases. On MR imaging, T2 hyperintensities with diffusion restrictions involve the cerebral cortex, hippocampus, SCC, internal capsule, and cerebral WM. Cytotoxic edema due to excitotoxic brain injury leads to diffusion restrictions (Fig. 7) (17). The central portion of the SCC has abundant glutamate receptors and high enzymatic activity (18, 19). Because of these histologic features, it is affected by hypoglycemia.

CO-Intoxication

CO-intoxication shows various distributions based on the severity of insult and time of imaging. The globus pallidus is the most commonly affected region. It may also involve the cerebral WM, sparing subcortical fiber. Cerebral

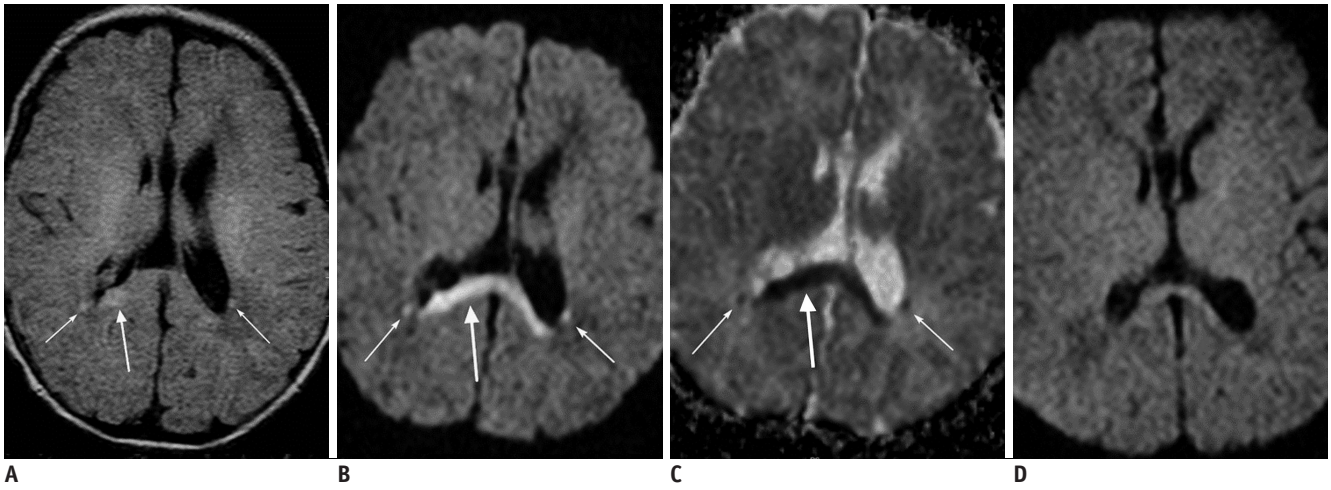

Fig. 6. 8-day-old female patient with hypoxic-ischemic encephalopathy. Patient had birth asphyxia.
A, B. Axial FLAIR image **(A)** and DWI **(B)** show hyperintense lesions in splenium of corpus callosum (thick arrows) and bilateral posterior deep periventricular white matter (thin arrows). **C.** ADC map image reveals restricted water diffusion of lesions (arrows). **D.** Follow-up axial DWI image obtained 1 month later shows decrease in signal intensity of lesions. ADC = apparent diffusion coeffcient, DWI = diffusion-weighted image, FLAIR = fluid-attenuated inversion recovery

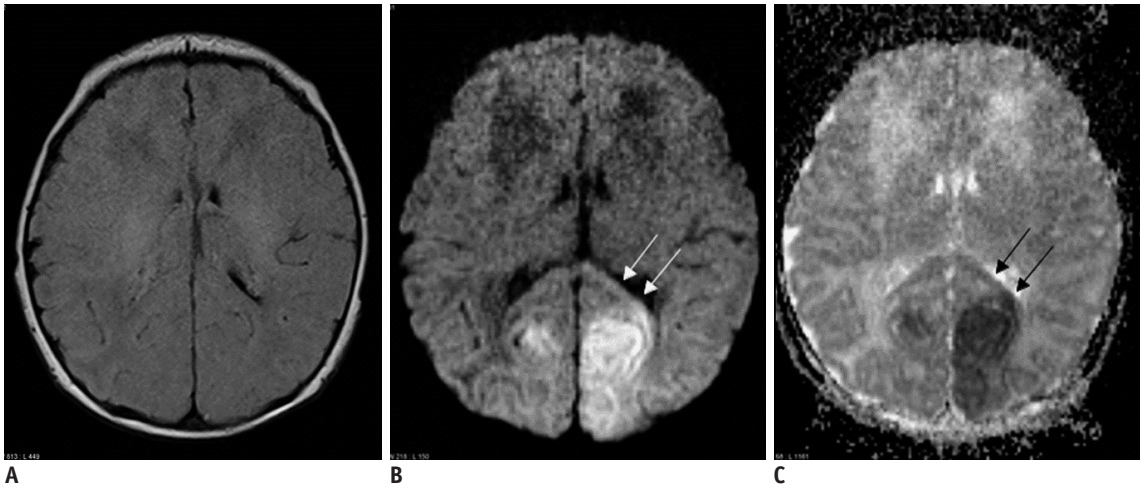

Fig. 7. 2-day-old female with hypoglycemic encephalopathy. Glucose level was 2 mg/dL at presentation.
A. On FLAIR axial image, there is no definite lesion. **B.** Axial DWI shows hyperintense lesions in both occipital lobes and splenium (arrows). **C.** ADC map image reveals restricted water diffusion of lesions (arrows). ADC = apparent diffusion coeffcient, DWI = diffusion-weighted image, FLAIR = fluid-attenuated inversion recovery

Korean Journal of Radiology
KJR

WM damage can be observed in the centrum semiovale, periventricular WM, and CC including the splenium. As in hypoglycemic encephalopathy, the cerebellum and brain stem are usually spared in CO poisoning. In the acute stage, affected areas show bilateral low signal intensity on T1 and high signal intensity on T2-weighted images. DWI shows restriction of water diffusion due to cytotoxic edema (Fig. 8). Hemorrhagic necrosis in the globus pallidus appears as dark signal intensity on the GRE T2*-weighted image. In the late stage, CO-intoxication can cause diffuse brain atrophy and cerebral WM demyelination (20, 21).

Tumors

Lymphoma

Lesions of the CC are typically aggressive, as the CC is composed of very dense WM tracts that act like a barrier to tumor spreading (22). The main differential diagnosis for a splenial tumor is primary lymphoma and glioblastoma, which tend to extend across the midline into the opposite hemisphere.

Primary central nervous system (CNS) lymphomas are rare aggressive neoplasms and almost always the B-cell

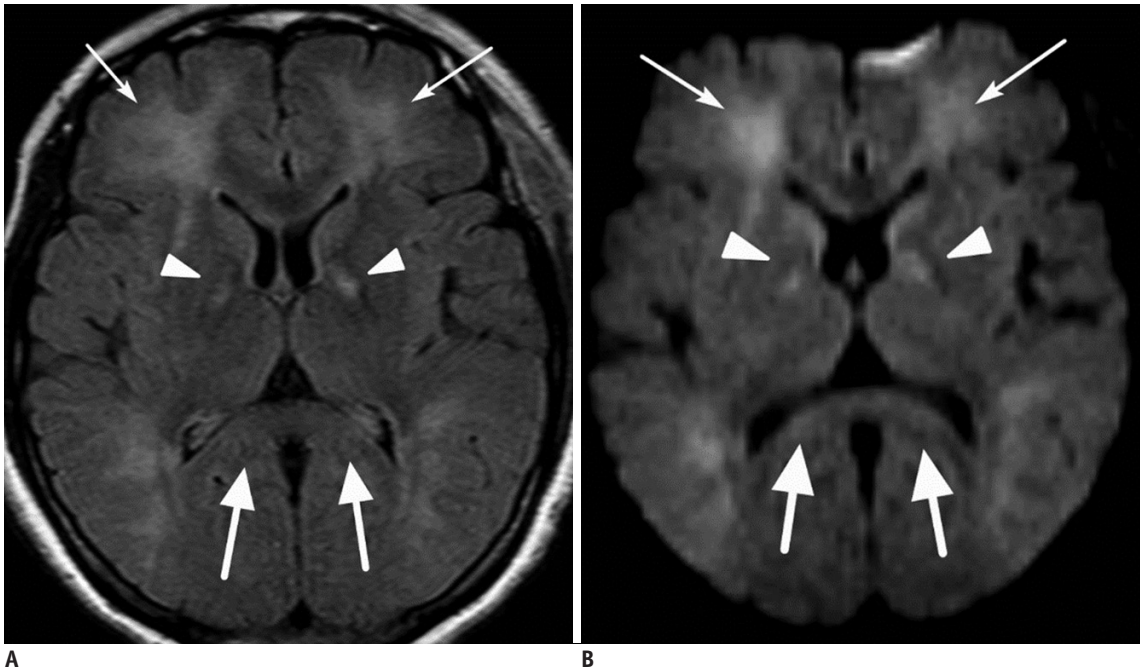

A B

Fig. 8. 48-year-old female patient with CO-intoxication.
Axial FLAIR image **(A)** and DWI **(B)** show multiple hyperintense lesions in bilateral globus pallidus (arrowheads) and cerebral white matter (thin arrows) including splenium of corpus callosum (thick arrows). DWI = diffusion-weighted image, FLAIR = fluid-attenuated inversion recovery

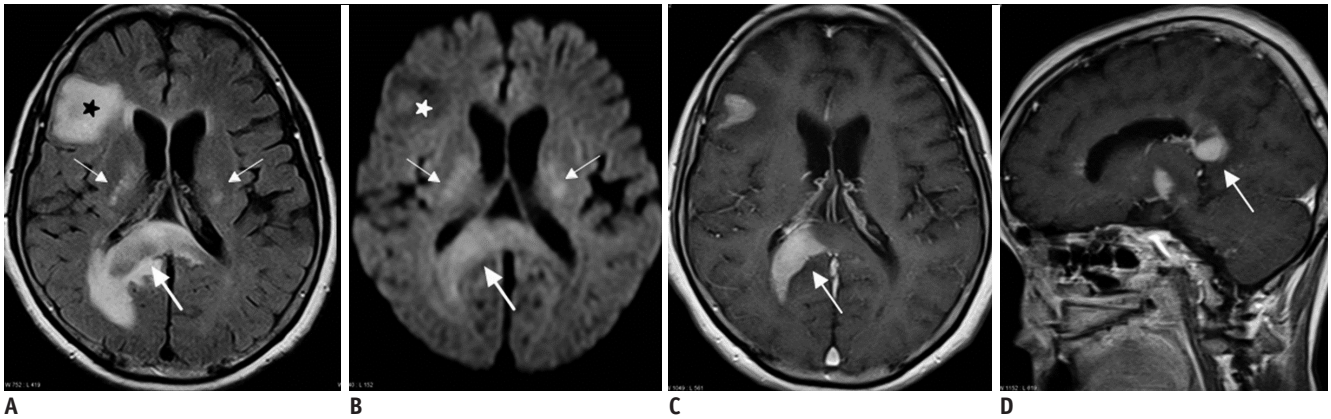

A B C D

Fig. 9. 61-year-old female patient with lymphomas.
A, B. Axial FLAIR image **(A)** and DWI **(B)** show multiple hyperintense lesions in bilateral basal ganglia (thin arrows), splenium (thick arrows), and right frontal lobe (stars). **C, D.** On enhanced T1-weighted axial **(C)** and sagittal **(D)** images, splenial lesion (thick arrows) is homogeneously enhanced. DWI = diffusion-weighted image, FLAIR = fluid-attenuated inversion recovery

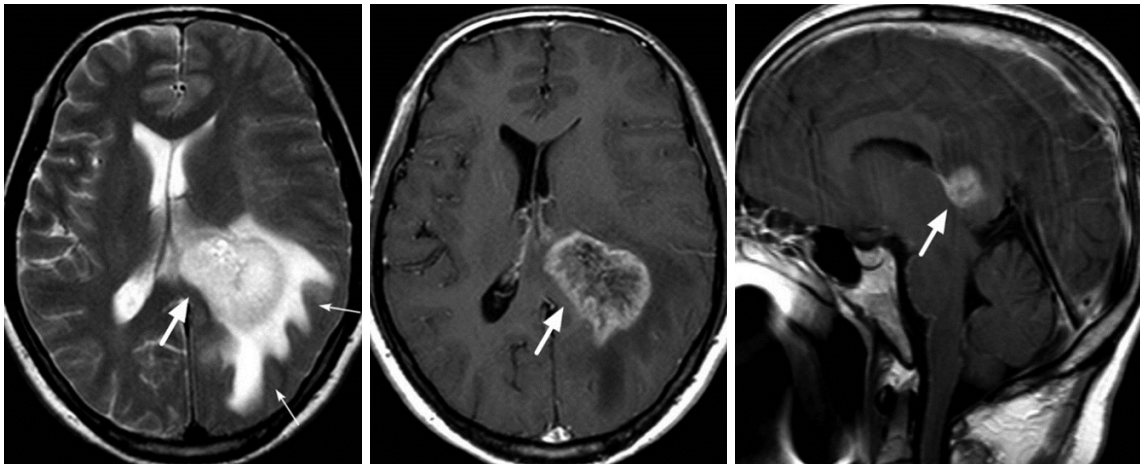

A B C

Fig. 10. 52-year-old male patient with glioblastoma.
A. Axial T2-weighted image shows large hyperintense mass in left deep periventricular white matter and adjacent splenium of corpus callosum (thick arrow). There is large amount of surrounding brain edema (thin arrows). **B, C.** On enhanced T1-weighted axial **(B)** and sagittal **(C)** images, mass is strongly enhanced (thick arrows).

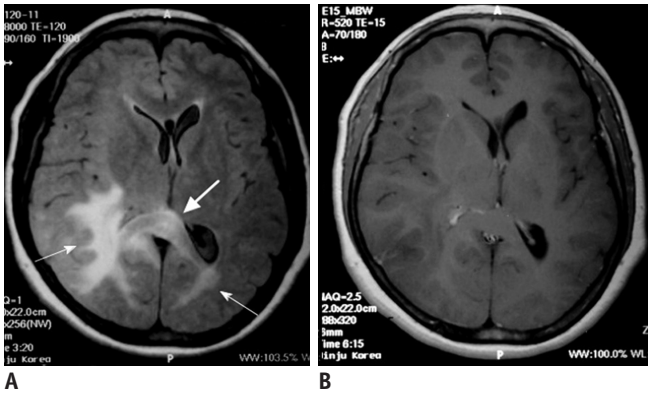

A B

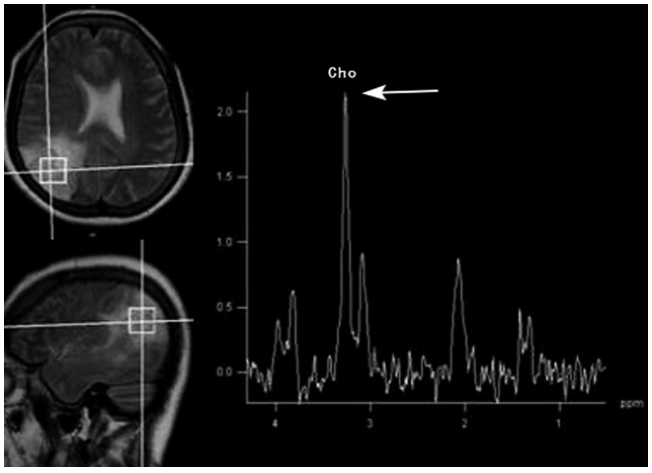

C

Fig. 11. 46-year-old female patient with gliomatosis cerebri.
A. Axial FLAIR image shows ill-defined hyperintense lesions involving bilateral posterior cerebral white matter (thin arrows) and splenium of corpus callosum (thick arrow). **B.** Enhanced T1-weighted axial image shows no definite contrast enhancement of lesion. **C.** Single voxel 1H MR spectroscopy reveals increased choline peak (thick arrow). FLAIR = fluid-attenuated inversion recovery

non-Hodgkin's type. Common locations of CNS lymphoma include the CC, deep gray matter, and periventricular WM region. Lymphomas are commonly multifocal and nodular. Typically, lymphoma is isointense or hypointense on T1 and slightly hyperintense or isointense relative to gray matter on T2-weighted image. On DWI, it shows restricted water diffusion, reflective of dense cellularity (23). There is usually homogeneous enhancement on contrast study. These features are useful in the differential diagnosis of lymphoma from glioblastoma (Fig. 9).

Glioma

Glioblastoma is the most common and aggressive diffuse astrocytic tumor in the brain. Glioblastoma commonly spread along WM tract, including the splenium. Glioblastoma has typically bihemispheric involvement with infiltration of the CC, resulting in a butterfly pattern. Therefore, when any lesion crosses the CC, glioblastoma should be considered. On MR, the tumor shows heterogeneously low signal intensity on T1 and high signal intensity on T2-weighted images with irregular contrast enhancement. Solid portions of the tumor demonstrate restricted diffusion, suggesting high cellularity. Peritumoral vasogenic edema, mass effect and internal necrosis are usually prominent (Fig. 10) (15, 22).

Gliomatosis cerebri, a slow growing and diffuse infiltrative form of glioma, involves at least three lobes of the cerebrum, and may also affect the SCC. Gliomatosis cerebri was previously considered a distinct entity; however, since the 2016 update to the World Health Organization classification of CNS tumors it is considered a growth

Korean Journal of Radiology
KJR

pattern. Contrary to glioblastoma, gliomatosis cerebri shows less mass effect and minimal contrast enhancement. MR features of gliomatosis cerebri include isointensity to hypointensity on T1 and hyperintensity on T2-weighted images (Fig. 11) (15).

Fig. 12. 32-year-old male patient with pineal germinoma.
Enhanced T1-weighted sagittal image shows strong enhancing mass in pineal gland area. Mass extends into 3rd ventricle anteriorly and invades splenium of corpus callosum (arrow) and tectum inferiorly.

Germinoma

Germinoma tends to occur in the midline, either at the pineal region or along the inferior surface or the third ventricle/suprasellar region. The floor of the CC can be involved with ependymal and subependymal dissemination (9). Pineal germinoma may extend directly into the SCC superiorly and the tectum inferiorly (Fig. 12).

Degenerative and Demyelinating Disease

Wallerian Degeneration

Wallerian degeneration is defined as distal axonal degeneration after transection or crushing of the nerve trunk itself. Wallerian degeneration is rarely seen in the SCC. For example, posterior cerebral artery territory infarction can produce atrophy of the SCC. This atrophy is related to wallerian degeneration of commissural fibers (Fig. 13). DWI is a good technique for early detection of callosal degeneration. And diffusion tensor MR imaging is more sensitive than the morphologic MR imaging for the evaluation of wallerian degeneration in the CC (24).

Multiple Sclerosis

Multiple sclerosis (MS) is inflammatory demyelinating disease of idiopathic cause. Lesions characteristically involve the periventricular WM, internal capsule, CC, and

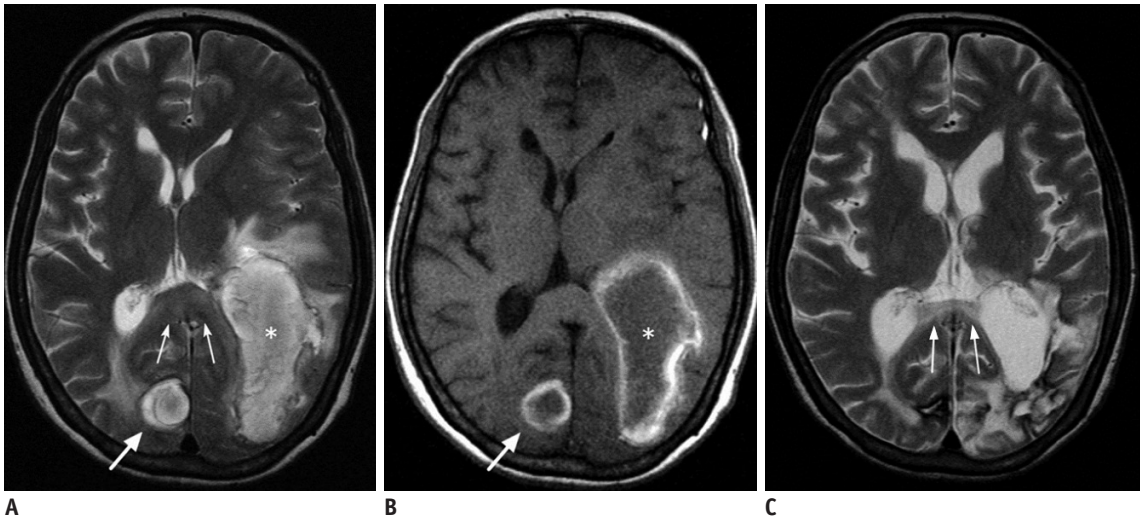

Fig. 13. 49-year-old female patient with Wallerian degeneration due to intracerebral hematomas.
A, B. Axial T2 **(A)** and T1-weighted **(B)** images show two hyperintense hematomas in right occipital lobe (thick arrows) and left temporooccipital lobes (asterisks). There is moderate amount of surrounding brain edema. Splenium also shows mild swelling and increased signal intensity (thin arrows). **C.** Follow-up T2-weighted image obtained 20 months later reveals atrophic change and increased signal intensity of splenium (thin arrows).

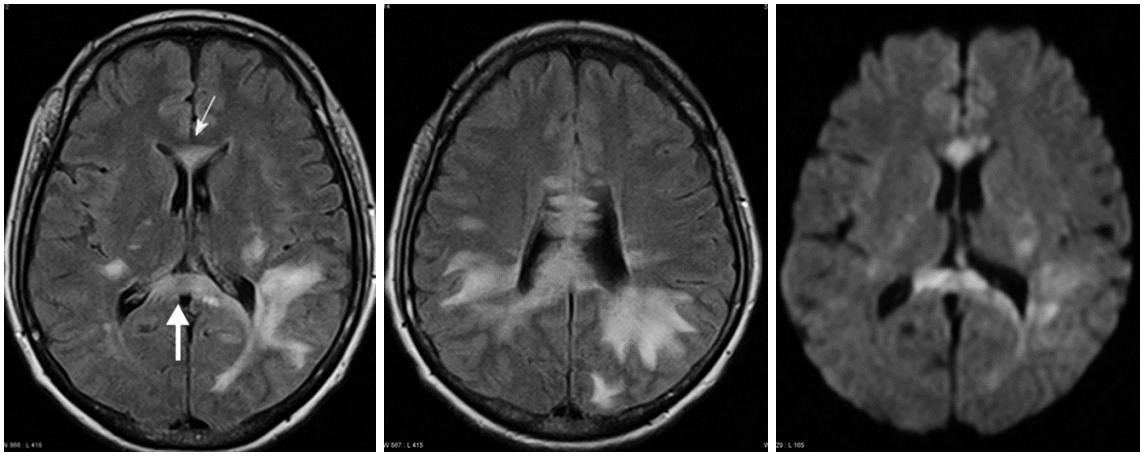

Fig. 14. 39-year-old female patient with multiple sclerosis.
A, B. Axial FLAIR images show multiple hyperintense lesions in both periventricular white matter, genu (thin arrow), and splenium (thick arrow) of corpus callosum. **C.** On DWI, most of lesions are demonstrated as hyperintensities. DWI = diffusion-weighted image, FLAIR = fluid-attenuated inversion recovery

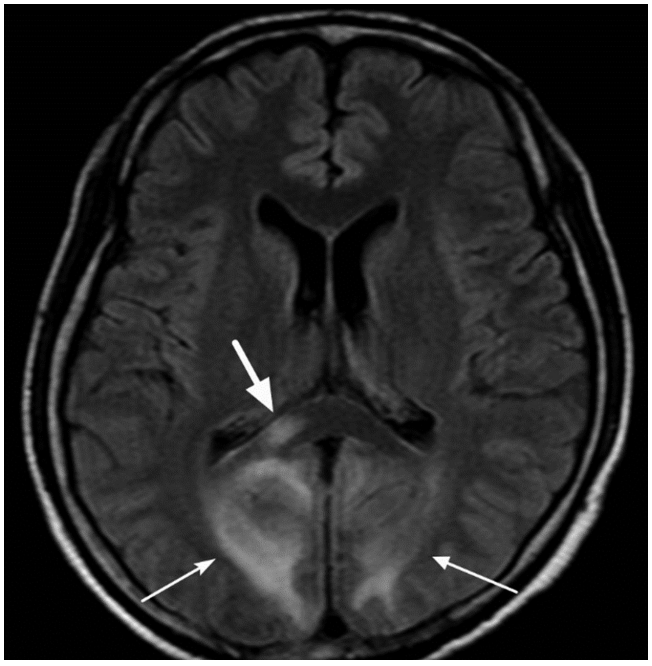

Fig. 15. 29-year-old female patient with posterior reversible encephalopathy syndrome due to eclampsia. Axial FLAIR image shows multiple hyperintense lesions in cortices and white matter of both occipital lobes (thin arrows). There is also focal hyperintense lesion in right portion of splenium (thick arrow). FLAIR = fluid-attenuated inversion recovery

pons. The prevalence of lesions in the CC has been reported as up to 90% in the radiology literature. Although round or oval lesions commonly involve the callosal-septal interface, the splenium can also be affected. And mostly, the lesions accompany deep WM lesions rather than solitary involvement of the SCC. MS can appear as subtle diffuse hyperintensity on T2 and hypointensity on T1-weighted images. On DWI, they show variable signal intensities (Fig. 14). In the acute active stage, lesions can be revealed in enhancement study. Atrophy is common with progression of the disease (22).

Acute Disseminated Encephalomyelitis

Acute disseminated encephalomyelitis (ADEM) is a post-infectious immune-mediated inflammatory demyelinating condition that predominately affects the WM of the brain and spinal cord. Typical lesions of ADEM include centrifugal at the junction of the deep cortical gray and subcortical WM. MR imaging features are like those of MS. However, periventricular and CC lesions are uncommon in pediatric ADEM, as compared with MS (25).

Posterior Reversible Encephalopathy Syndrome

Posterior reversible encephalopathy syndrome (PRES) is characterized by headache, confusion, seizures, and visual loss; it is accompanied by symmetric parietooccipital edema on imaging. PRES may show bilateral high intensities involving the subcortical WM of the parietal and occipital lobes on T2-weighted image. DWI usually shows the lesions as isointensities with increased water diffusion. Atypical distributions of PRES have a higher incidence than commonly perceived. Bartynski and Boardman (26) reported that the cerebellum (32%), basal ganglia (14%), brain stem (13%), and deep WM (18%) including the SCC (10%) could be affected (Fig. 15).

Korean Journal of Radiology
KJR

Toxic Encephalopathy

Marchiafava-Bignami Disease

Marchiafava-Bignami disease is a primary degenerative disease of the CC in chronic alcoholics or poorly nourished nondrinkers. It is attributed to a deficiency of vitamin B complex and results in necrosis and demyelination of the CC. The disease typically begins in the body of the CC and later involves the genu and splenium (27). MR imaging may show swelling of CC with high intensity on T2-weighted image and often enhances in the acute stage, thought to represent edema and demyelination, and atrophic change in the chronic stage (Fig. 16).

Metronidazole-Induced Encephalopathy

Metronidazole-induced encephalopathy (MIE) is a rare disease caused by adverse effects of the antibiotic drug. Lesions of MIE are typically located at the cerebellar dentate nucleus, midbrain, dorsal pons, medulla, and SCC bilaterally and symmetrically. The lesions appear as non-enhancing, hyperintense on T2 and fluid attenuated inversion recovery (FLAIR) images without evidence of mass effect. Based on DWI, most of the lesions in MIE probably correspond to areas of vasogenic edema, whereas only some of them, located in the SCC, correspond to cytotoxic edema. Despite the many possible differential diagnoses such as

Fig. 16. 59-year-old male patient with chronic alcoholism.
A, B. FLAIR **(A)** and T2-weighted **(B)** images show hyperintense lesions in body (thin arrows) and splenial portion (thick arrows) of corpus callosum. **C.** There is focal contrast enhancement of lesions (arrows) on post-contrast T1-weighted image. FLAIR = fluid-attenuated inversion recovery

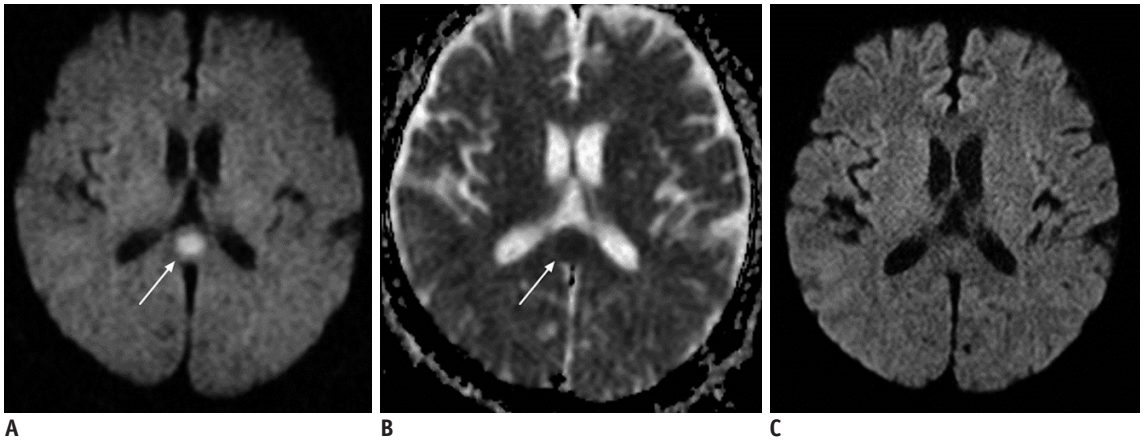

Fig. 17. 62-year-old male patient with epilepsy.
A. Axial DWI shows focal hyperintense lesion in splenium of corpus callosum (arrow). **B.** ADC map image reveals restricted water diffusion of lesion (arrow). **C.** On follow-up DWI obtained 14 days later, splenial lesion has disappeared. ADC = apparent diffusion coeffcient, DWI = diffusion-weighted image

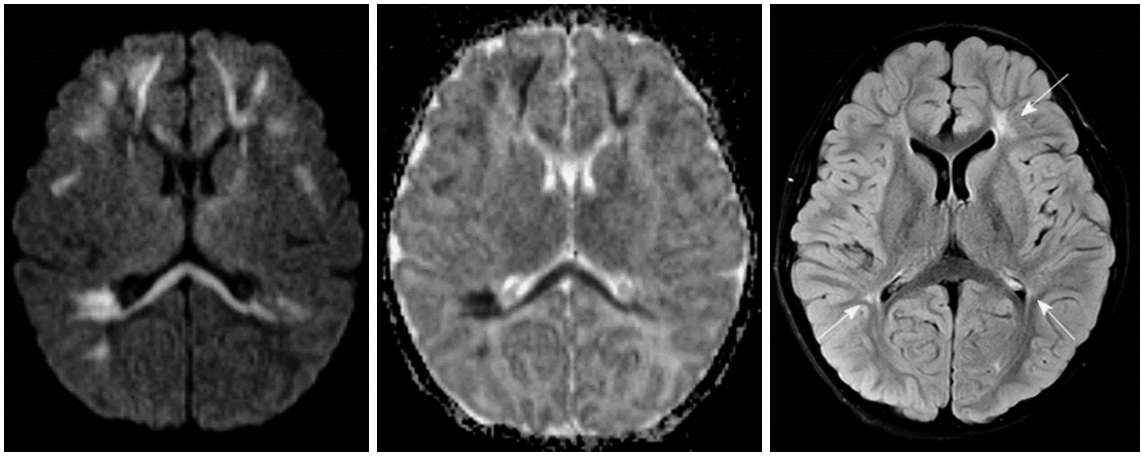

Fig. 18. 5-day-old male with rotavirus-related white matter injury.
A, B. Initial axial DWI **(A)** and ADC map **(B)** demonstrate extensive areas of restricted diffusion in periventricular white matter, deep white matter, corpus callosum, internal capsule, and posterior thalami. **C.** Follow-up FLAIR image obtained five years later shows residual ischemic lesions due to previous white matter injury in both periventricular white matters (arrows). ADC = apparent diffusion coeffcient, DWI = diffusion-weighted image, FLAIR = fluid-attenuated inversion recovery

MS, Wernicke encephalopathy and Marchiafava-Bignami disease, toxicity in cases can be suspected in the presence of the characteristic distribution of lesions, bilaterally symmetric, with involvement of the cerebellar dentate nuclei in most cases, and confirmed when the characteristic history of metronidazole intake is available and on reversal of symptoms and MRI findings after cessation of drug intake (28).

Miscellaneous Lesions

Transient Lesion of the Splenium

Transient lesion of the central splenium has been reported in conditions with varied etiologies, including epilepsy, the usage as well as sudden withdrawal of antiepileptic drugs, infections including influenza, HIV and tuberculous meningitis and other conditions like hemolytic-uremic syndrome (29). Transient lesions of the splenium are only readily detectable on MR as two distinct patterns: well circumscribed, small, oval lesions in the midline within the splenium; or more extensive less regular lesions extending throughout the splenium and into the adjacent hemispheres. The smaller well circumscribed lesions are the typical lesion seen in the setting of seizures/cessation of antiepileptic medication; whereas, the larger lesions are more typical of other etiologies (30, 31). These splenial lesions tend to demonstrate hyperintense on T2 and FLAIR images and iso- or hypointense on T1-weighted image without enhancement. The changes in DWI appear earlier than the changes in T2 and FLAIR images. MR studies have shown that patients recover completely within 1 month, mostly within 1 week following the neurologic recovery (Fig. 17).

White Matter Injury in Neonatal Viral Infection

Recently, extensive WM injury has been reported in neonates with viral infections such as parechovirus and rotavirus (32, 33). Although clinical signs and symptoms and laboratory findings differ between parechovirus and rotavirus, they show identical MR findings. MR features are characterized by symmetrical restricted diffusion in the periventricular and subcortical WM, CC, internal and external capsules, and pyramidal tracts of the supratentorial brain and cerebral peduncle (Fig. 18).

CONCLUSION

From congenital to acquired lesions, various diseases can involve the splenium of the CC. Knowledge of their categories and imaging features can be helpful for the appropriate approach to the SCC lesions.

REFERENCES

1. Lee SK, Kim DI, Kim J, Kim DJ, Kim HD, Kim DS, et al. Diffusion-tensor MR imaging and fiber tractography: a new method of describing aberrant fiber connections in developmental CNS anomalies. *Radiographics* 2005;25:53-65; discussion 66-68
2. Doherty MJ, Jayadev S, Watson NF, Konchada RS, Hallam DK.

Clinical implications of splenium magnetic resonance imaging signal changes. *Arch Neurol* 2005;62:433-437
3. Park MK, Hwang SH, Jung S, Hong SS, Kwon SB. Lesions in the splenium of the corpus callosum: clinical and radiological implications. *Neurol Asia* 2014;19:79-88
4. Li S, Sun X, Bai YM, Qin HM, Wu XM, Zhang X, et al. Infarction of the corpus callosum: a retrospective clinical investigation. *PLoS One* 2015;10:e0120409
5. Georgy BA, Hesselink JR, Jernigan TL. MR imaging of the corpus callosum. *AJR Am J Roentgenol* 1993;160:949-955
6. Barkovich AJ, Norman D. Anomalies of the corpus callosum: correlation with further anomalies of the brain. *AJR Am J Roentgenol* 1988;151:171-179
7. Truwit CL, Barkovich AJ. Pathogenesis of intracranial lipoma: an MR study in 42 patients. *AJR Am J Roentgenol* 1990;155:855-864; discussion 865
8. Ginat DT, Meyers SP. Intracranial lesions with high signal intensity on T1-weighted MR images: differential diagnosis. *Radiographics* 2012;32:499-516
9. Uchino A, Takase Y, Nomiyama K, Egashira R, Kudo S. Acquired lesions of the corpus callosum: MR imaging. *Eur Radiol* 2006;16:905-914
10. Provenzale JM. Imaging of traumatic brain injury: a review of the recent medical literature. *AJR Am J Roentgenol* 2010;194:16-19
11. Arfanakis K, Haughton VM, Carew JD, Rogers BP, Dempsey RJ, Meyerand ME. Diffusion tensor MR imaging in diffuse axonal injury. *AJNR Am J Neuroradiol* 2002;23:794-802
12. Scheid R, Preul C, Gruber O, Wiggins C, von Cramon DY. Diffuse axonal injury associated with chronic traumatic brain injury: evidence from T2*-weighted gradient-echo imaging at 3 T. *AJNR Am J Neuroradiol* 2003;24:1049-1056
13. Chrysikopoulos H, Andreou J, Roussakis A, Pappas J. Infarction of the corpus callosum: computed tomography and magnetic resonance imaging. *Eur J Radiol* 1997;25:2-8
14. Kasow DL, Destian S, Braun C, Quintas JC, Kagetsu NJ, Johnson CE. Corpus callosum infarcts with atypical clinical and radiologic presentations. *AJNR Am J Neuroradiol* 2000;21:1876-1880
15. Ho ML, Moonis G, Ginat DT, Eisenberg RL. Lesions of the corpus callosum. *AJR Am J Roentgenol* 2013;200:W1-W16
16. Chao CP, Zaleski CG, Patton AC. Neonatal hypoxic-ischemic encephalopathy: multimodality imaging findings. *Radiographics* 2006;26 Suppl 1:S159-S172
17. Auer RN. Hypoglycemic brain damage. *Metab Brain Dis* 2004;19:169-175
18. Kang EG, Jeon SJ, Choi SS, Song CJ, Yu IK. Diffusion MR imaging of hypoglycemic encephalopathy. *AJNR Am J Neuroradiol* 2010;31:559-564
19. Beltran-Marin M, Sadeghi N. Transient restricted diffusion in the splenium of the corpus callosum after brain surgery. *JBR-BTR* 2013;96:92
20. Lo CP, Chen SY, Lee KW, Chen WL, Chen CY, Hsueh CJ, et al. Brain injury after acute carbon monoxide poisoning: early and late complications. *AJR Am J Roentgenol* 2007;189:W205-W211
21. Beppu T. The role of MR imaging in assessment of brain damage from carbon monoxide poisoning: a review of the literature. *AJNR Am J Neuroradiol* 2014;35:625-631
22. Bourekas EC, Varakis K, Bruns D, Christoforidis GA, Baujan M, Slone HW, et al. Lesions of the corpus callosum: MR imaging and differential considerations in adults and children. *AJR Am J Roentgenol* 2002;179:251-257
23. Kim M, Kim HS. Emerging techniques in brain tumor imaging: what radiologists need to know. *Korean J Radiol* 2016;17:598-619
24. Gupta RK, Saksena S, Hasan KM, Agarwal A, Haris M, Pandey CM, et al. Focal Wallerian degeneration of the corpus callosum in large middle cerebral artery stroke: serial diffusion tensor imaging. *J Magn Reson Imaging* 2006;24:549-555
25. Brass SD, Caramanos Z, Santos C, Dilenge ME, Lapierre Y, Rosenblatt B. Multiple sclerosis vs acute disseminated encephalomyelitis in childhood. *Pediatr Neurol* 2003;29:227-231
26. Bartynski WS, Boardman JF. Distinct imaging patterns and lesion distribution in posterior reversible encephalopathy syndrome. *AJNR Am J Neuroradiol* 2007;28:1320-1327
27. Arbelaez A, Pajon A, Castillo M. Acute Marchiafava-Bignami disease: MR findings in two patients. *AJNR Am J Neuroradiol* 2003;24:1955-1957
28. Kim E, Na DG, Kim EY, Kim JH, Son KR, Chang KH. MR imaging of metronidazole-induced encephalopathy: lesion distribution and diffusion-weighted imaging findings. *AJNR Am J Neuroradiol* 2007;28:1652-1658
29. Hirotani M, Yabe I, Hamada S, Tsuji S, Kikuchi S, Sasaki H. Abnormal brain MRI signals in the splenium of the corpus callosum, basal ganglia and internal capsule in a suspected case with tuberculous meningitis. *Intern Med* 2007;46:505-509
30. Conti M, Salis A, Urigo C, Canalis L, Frau S, Canalis GC. Transient focal lesion in the splenium of the corpus callosum: MR imaging with an attempt to clinical-physiopathological explanation and review of the literature. *Radiol Med* 2007;112:921-935
31. Malhotra HS, Garg RK, Vidhate MR, Sharma PK. Boomerang sign: clinical significance of transient lesion in splenium of corpus callosum. *Ann Indian Acad Neurol* 2012;15:151-157
32. Yeom JS, Kim YS, Seo JH, Park JS, Park ES, Lim JY, et al. Distinctive pattern of white matter injury in neonates with rotavirus infection. *Neurology* 2015;84:21-27
33. Amarnath C, Helen Mary T, Periakarupan A, Gopinathan K, Philson J. Neonatal parechovirus leucoencephalitis-radiological pattern mimicking hypoxic-ischemic encephalopathy. *Eur J Radiol* 2016;85:428-434